DEFECT SIZING IN PIPE USING AN ULTRASONIC GUIDED WAVE FOCUSING TECHNIQUE

Jing Mu[1], Li Zhang[1], Joseph L. Rose[1] and Jack Spanner[2]

[1]Department of Engineering Science and Mechanics, The Pennsylvania State University, University Park, PA 16802
[2]EPRI NDE Center, 1300 WT Harris Blvd., Charlotte, NC 28262

ABSTRACT. Defect circumferential location, circumferential length and depth are studied with an ultrasonic guided wave focusing inspection technique. Differently shaped defects, such as a planar saw cut, a volumetric through-wall hole, and a volumetric spherical shape corrosion are studied. By focusing on 44 circumferential positions around the pipe at a specific distance, the maximum amplitude of the defect echo is recorded with respect to each circumferential focal position. Circumferential lengths of the planar saw cut and volumetric through-wall hole are then measured by comparing the experimental results with theoretical calculations. It is shown that this measurement technique works well with the planar saw cut and volumetric through-wall hole defects. In addition, it is shown that reflections from defects with the same cross sectional area (CSA), but different shapes, might be very different.

Keywords: circumferential defect sizing, ultrasonic guided waves, focusing.
Pacs: 43.20.Mv, 43.20.Ks, 43.20.Ye.

INTRODUCTION

Guided waves have been widely used for over ten years. Guided waves can propagate a long distance and are excellent in screening and defect location analysis. The state of the art of guided waves utilization defect sizing is limited. A beautiful result of 2D defects in a plate has already been obtained [1]. Similar results are also expected in pipes. However, since the somewhat ellipsoidal corrosion in pipe is 3D, defect sizing in pipes is more complicated. The focusing technique developed by Li and Rose [2] is used to increase the detection potential and to achieve a sizing possibility.

In this paper, guided wave experiments were performed to detect and study defect circumferential location, circumferential length and depth. The recently developed phased array focusing system [2-3] was utilized to focus on 44 circumferential positions around the pipe at a specific axial distance (defect location). This is called a circumferential scan. The pulse echo waveform for each focused position in one circumferential scan was then recorded. Since there is a focal zone, multiple defects lying in a focal zone were able to be detected in one circumferential scan.

A gate could be set according to the focal zone in each circumferential scan. The maximum amplitude in the gate in each of these waveforms was plotted with respect to the circumferential focused position. This produced an experimental circumferential profile.

CP820, *Review of Quantitative Nondestructive Evaluation Vol. 25,* ed. by D. O. Thompson and D. E. Chimenti

The profile was further used to study the defect's circumferential location, length and depth.

The reflected energy from a defect was considered to be proportional to the energy impinged on that defect. For each focused position, the energy impinged on a defect was calculated through the focused angular profile, which was obtained through the Normal Mode Expansion (NME) technique [4]. In this way, the impinging energy was able to be plotted with respect to the circumferential focused position. This gave us a theoretical energy impingement profile. The theoretical profiles for defects with different circumferential sizes were calculated and compared with the experimental pulse echo profile. Thus, the circumferential size of the defect could be measured.

Corrosion with different depths was also studied. The reflected energy showed an overall increasing potential of defect sizing analysis.

EXPERIMENTAL SETUP

Ultrasonic guided wave inspection was performed to detect and to study the circumferential location, length and depth of the defects in a 16" Schedule 30 pipe. The multi-channel commercial system TeleTest®, segmented over four quadrants or eight octants, as shown in Figure 1, was used to apply the phased array focusing technique. The defects are listed in Table 1. Ultrasonic energy was focused at z_1=10'11'', z_2=15'5'' and z_3=19'3'' by controlling input time delays and amplitudes for the 4 excitation channels. The frequency of the ultrasonic guided waves considered in the study varied over 30 kHz to 45 kHz.

LOCATING MULTIPLE DEFECTS IN ONE CIRCUMFERENTIAL SCAN

When ultrasonic guided wave energy is focused at a particular axial position, there is a focal zone, over which the energy is always focused on a predetermined circumferential location. For example, when we focus on 0° at the distance z=15'5'' using the T [0, 1] wave mode group at 35 kHz, the ultrasonic energy is focused at 0° over the axial range: 11'2''~19'6''. Based on this phenomenon, it is easy to verify a defect signal and then to axially locate the defect by arrival time analysis. A time gate can be set for the received signals and the maximum amplitude within this gate can be recorded when guided waves

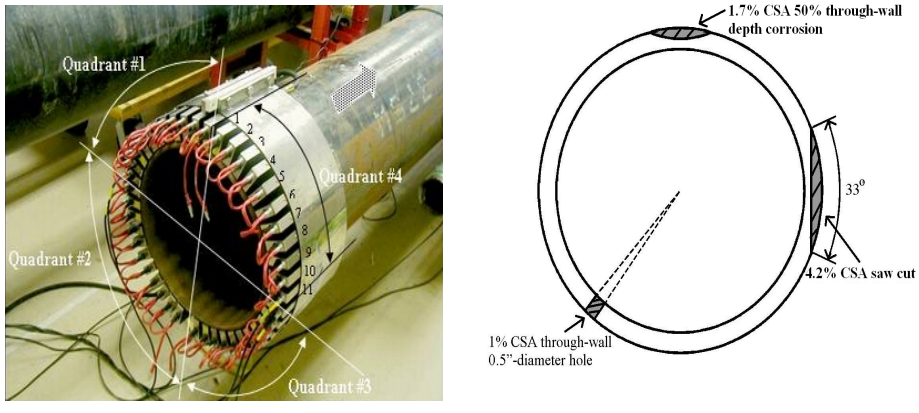

FIGURE 1. TeleTest® tool mounted on a 16" Schedule 30 steel pipe for quantification of the circumferential sizes of various defects. Quadrant designations (left) and the circumferential distributions of defects (right) are shown for reference.

TABLE 1. Descriptions of all defects used in the study.

Defect Type	Position from transducer	Circumferential position (CW)	depth	Circumferential length	Axial length	CSA
Corrosion 1	131in (10'11'')	0°	10%	0.893in (6.4°)	1.093in	0.12%
Corrosion 2	131in (10'11'')	0°	30%	1.66in (11.8°)	2.11in	0.68%
Corrosion 3	131in (10'11'')	0°	50%	2.51in (18°)	3.66in	1.71%
Corrosion 4	131in (10'11'')	0°	70%	2.51in (18°)	3.66in	2.4%
Through-wall hole	185in (15'5'')	220°	100%	0.5in	0.5in	1%
Saw cut 1	231in (19'3'')	90°	73% (7mm)	119mm, 4.69in (33.6°)	0.1in	4.18%
Saw cut 2	231in (19'3'')	90°	73% (7mm)	239mm, 9.4in (66°)	0.1in	11%
Saw cut 3	231in (19'3'')	90°	73% (7mm)	(93°)	0.1in	
Saw cut 4	231in (19'3'')	90°	73% (7mm)	(123°)	0.1in	

are used to focus on at a particular circumferential angle. The variation of the maximum signal amplitude will show the circumferential locations of the defects located within the focal zone. In this study, we set a gate included signals arriving from the 12'5''~20'8'' range. By sweeping the focal point along the circumferential direction, the experimental data clearly show that there are two defects over this distance range (the simulated corrosion was introduced later): one was ~ 0°; and the other was ~ 135° (Figures 2 and 3). As can be seen in Table 1, the through-wall hole at z = 15'5''ft is located at 0° and the saw cut defect at z = 19'3'' is located at 135°. Hence, by sweeping the circumferential focal position, we can verify and locate all defects within the focal zone.

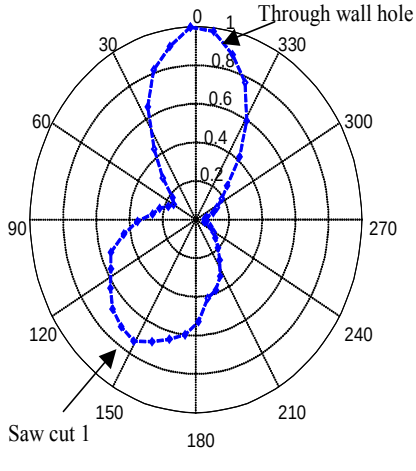

FIGURE 2. Maximum reflected echoes within the distance range: 12'5''~20'8'' when 4-channel phased-array was used to focus on the through-wall hole distance. The circumferential length of each excitation channel was 90°. The T [0, 1] wave group at 35 kHz was focused at 15'4'' and sequenced through 44 different circumferential locations.

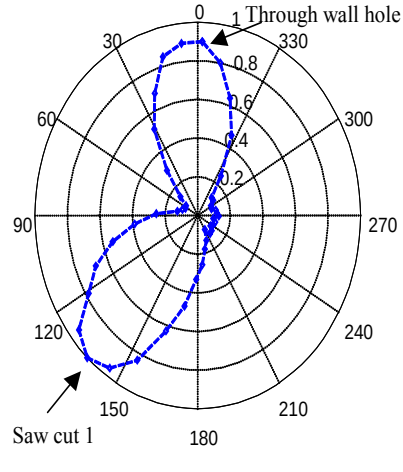

FIGURE 3. Maximum reflected echoes within the distance range: 12'5''~20'8'' when 4-channel phased-array was used to focus on the saw cut distance. The circumferential length of each excitation channel was 90°. The T [0, 1] wave group at 40 kHz was focused at 19'3'' and sequenced through 44 different circumferential locations.

DEFECT CIRCUMFERENTIAL AND DEPTH SIZING ANALYSIS

When a 4-channel phased array is used to achieve focusing, the circumferential excitation length of each channel would be approximately 90°. If the focal position is swept along the circumferential direction, the profiles of the energy impinging on the defect versus the focal angle can be obtained theoretically via the angular profile. For a planar defect, most of the impinging energy is reflected. Thus, a comparison of the experimental reflection profile and the theoretical energy impingement profiles provides us with the information on the circumferential size of the defect. The angular profile at 45 kHz is given in Figure 4 and the corresponding theoretical energy impingement profiles are given in Figure 5. It can be seen that the energy impingement profiles depend not only on the size of the defect but also on the shape of the corresponding angular profiles. If the angular profile exhibits a broad beam width or big side lobes, the corresponding energy impingement profiles will also exhibit a broad beam width or big side lobes. This is not good for sizing. However, since the shape of the angular profile changes with the distance, a certain frequency might be good for defect sizing at a certain distance.

In this study, by moving the focal point in the circumferential direction, 44 line of sight echoes from a defect could be recorded. The maximum amplitudes of the echoes are plotted versus the focal angles. This experimental reflection profile gave the variation of the reflected energy with respect to the focusing angle. The experimental and theoretical profiles for saw cuts with different circumferential sizes were compared as in Figure 6. The maximum amplitudes of the theoretical and experimental profiles of 33º circumferential length were normalized to the same value and the other profiles were normalized according to them. It's shown in Figure 6 that the profiles of the 66º circumferential length saw cut had larger amplitudes and wider circumferential coverage than that of the 33º circumferential length saw cut. This is obvious since for a longer saw cut, more energy is reflected and the 66º circumferential length saw cut can be seen from more focal positions out of the 44 used than the 33º circumferential length saw cut does. The corresponding

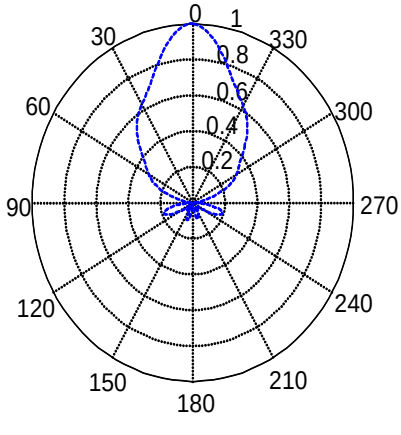

FIGURE 4. Theoretical angular profile of 45kHz focusing on 231in (saw cut distance).

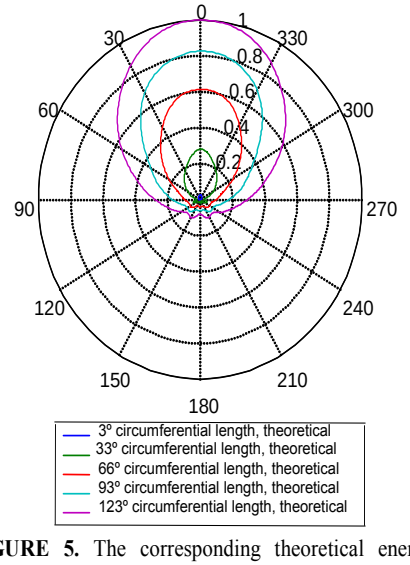

FIGURE 5. The corresponding theoretical energy impingement profiles for saw cuts with different circumferential sizes.

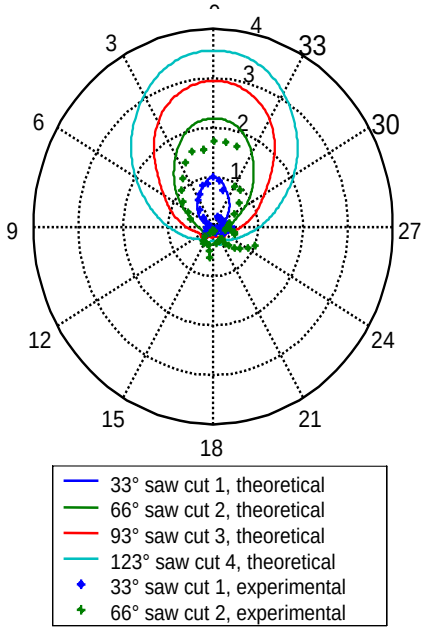

FIGURE 6. Comparison between theoretical and experimental profiles. The experimental profiles were obtained by applying 4-channel phased-array focusing. The T [0, 1] wave group at 45 kHz was focused on 44 different circumferential locations at 231 in.

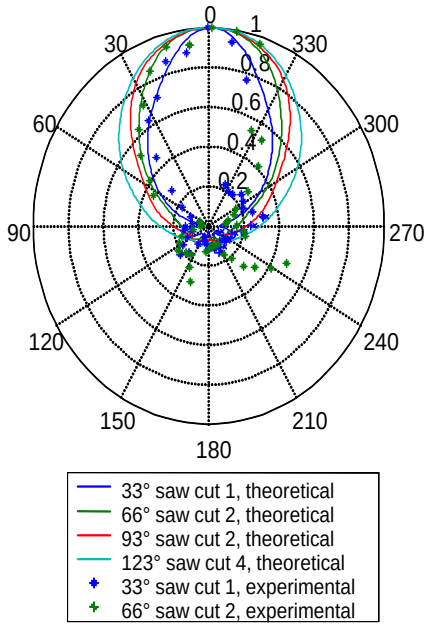

FIGURE 7. The experimental profiles of the defect echoes for saw cuts with different circumferential sizes are compared with the theoretical energy impingement profiles after normalization.

normalized profiles of Figure 6 are shown in Figure 7. It can be seen that the normalized theoretical profiles and the normalized experimental profiles match very well. Figure 7 can give a fairly good estimation on the circumferential size of a transverse crack.

For planar defects, the reflected energy is proportional to the energy impingement. To obtain quantitative defect sizing, the maximum amplitudes of the profiles can be calculated and plotted versus different circumferential sizes of the defects. This relation for saw cuts is shown in Figure 8. The theoretical results in Figure 8 were obtained from the theoretical energy impingement profiles in Figure 6. The maximum amplitude of each profile was recorded and plotted versus the corresponding circumferential size. This gave the theoretical result in Figure 8. The experimental results in Figure 8 were obtained from the experimental profiles in Figure 6. The maximum amplitude of the experimental defect echo profile in Figure 6 was recorded and plotted versus the corresponding circumferential size. The saw cuts with two different circumferential sizes 33º and 66º were measured, so two points were obtained, as shown in Figure 8. It can be seen that the experimental results match the theoretical calculations very well. The theoretical maximum amplitude increases monotonically with the increasing of the circumferential length. The relation is approximately linear. The slope of the line is related to the defect shape and the test frequency. The difference between the theoretical calculations and the experimental results is less than 10%.

The relation of the maximum amplitudes of the experimental profiles versus different depths of corrosion is plotted in Figure 9. For corrosion, there is a trend line that increases monotonically with corrosion defect depth. Note that the corrosion data is not perfectly linear because all corrosion is of slightly different shape. (If a transverse crack, the relationship would be more linear.)

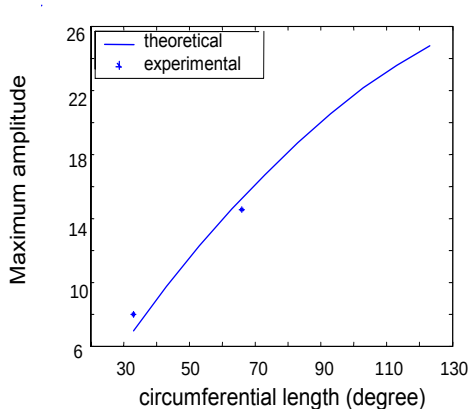

FIGURE 8. Monotonic increasing amplitude versus circumferential length for a fixed depth transverse saw cut at 45kHz.

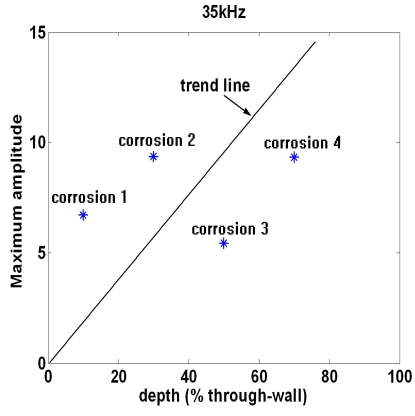

FIGURE 9. Possible variation of amplitude with depth for different corrosion defects at 35kHz.

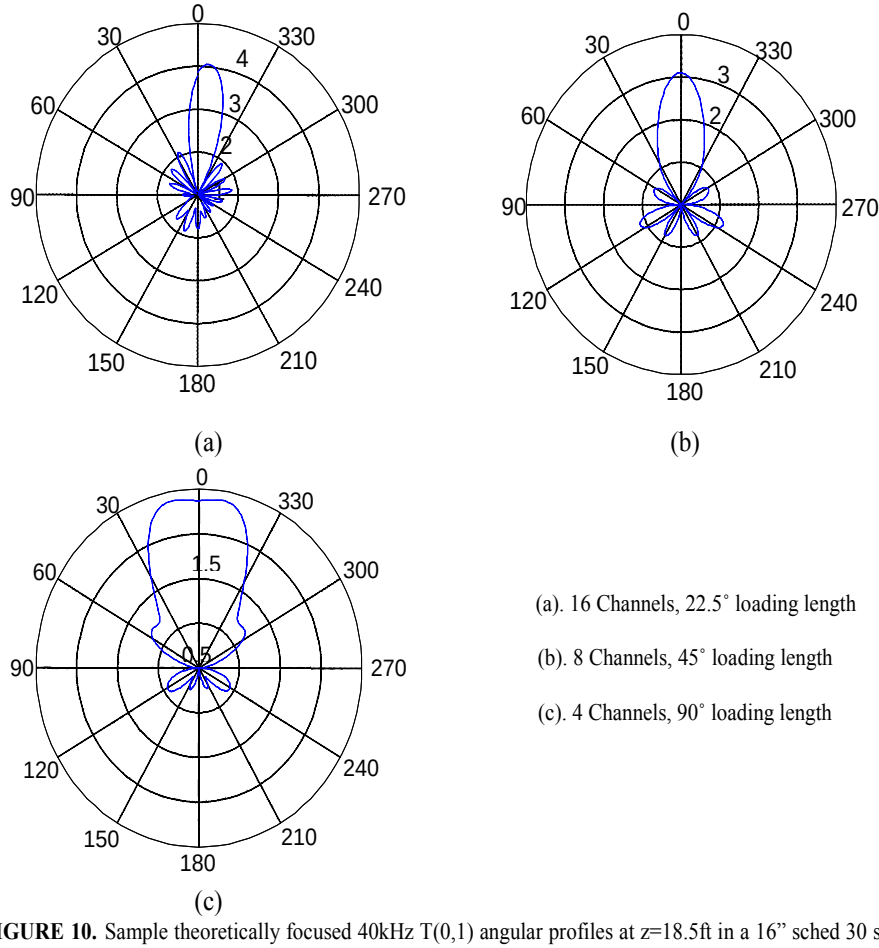

FIGURE 10. Sample theoretically focused 40kHz T(0,1) angular profiles at z=18.5ft in a 16" sched 30 steel pipe by using the phased array focusing technique with different loading lengths.

The focused angular profiles for different circumferential loading lengths are shown in Figure 10. Usually, the size of a focused beam is reduced with a decrease of

circumferential length of the excitation channels (Figure 10). It can be seen that the smallest defect size that can be determined by this technique depends on the focused energy beam characteristics. A narrower profile energy beam is able to be used to measure smaller defects.

CONCLUSIONS AND DISCUSSIONS

In this study, a long range ultrasonic guided wave test system was used to measure the circumferential size of volumetric corrosion defects and a transverse saw cuts by sweeping the focal position around the pipe. The circumferential location was determined very accurately for both saw cuts and corrosion defects. More precise circumferential length measurements can be obtained by comparing the experimental profiles with the theoretical energy impingement profiles. The maximum amplitude of the circumferential distribution profile matched the theoretical slope very well. It showed a monotonically increasing trend with circumferential length. The error was less than 10%. For the depth study, the maximum amplitude of the circumferential distribution profile of a corrosion defect did not increase monotonically with depth since all the corrosion defects had different shapes. However, it did show a possible overall increasing trend with depth. A narrower focal beam could make measurements more accurate. Both the shape of a defect and the shape of the angular profile will influence the predicted sizing results. Angular profiles with large side lobes are not good for defect sizing.

ACKNOWLEDGMENTS

Thanks are given to Peter Mudge at Plant Integrity, Ltd. for use of the Teletest® system, for support of the project to Mike J. Avioli of FBS, Inc., and to EPRI for financial support.

REFERENCES

1. Zhao, X. and Rose J. L., "Boundary element modeling for defect characterization potential in a wave guide," *International Journal of Solids Structures*, **40**, 2645-2658, 2003.
2. Li, J., and Rose, J.L., 2001, “Excitation and Propagation of Non-axisymmetric Guided Waves in a Hollow Cylinder,” *JASA*, **109**, pp. 457-464.
3. Li, J., and Rose, J. L., 2002, “Angular-Profile Tuning of Guided Waves in Hollow Cylinders Using a Circumferential Phased Array”, *IEEE Transactions on Ultrasonics, Ferroelectrics, and Frequency Control*, **49**, pp. 1720-1729.
4. Ditri, J. J., and Rose, J. L., 1992, “Excitation of guided elastic wave modes in hollow cylinders by applied surface tractions”, *J. Appl. Phys.*, **72**, 2589-2597.